Available online at www.sciencedirect.com
ScienceDirect
Polymer 48 (2007) 6311–6318
polymer
www.elsevier.com/locate/polymer

Porous poly(L-lactic acid) nanocomposite scaffolds prepared by phase inversion using supercritical CO_2 as antisolvent

Ioannis Tsivintzelis [a], Sotirios I. Marras [a,b], Ioannis Zuburtikudis [b], Costas Panayiotou [a,*]

[a] *Department of Chemical Engineering, Aristotle University of Thessaloniki, 54124 Thessaloniki, Greece*
[b] *Department of Industrial Design Engineering, TEI of Western Macedonia, 50100 Kozani, Greece*

Received 16 April 2007; received in revised form 13 July 2007; accepted 4 August 2007
Available online 14 August 2007

Abstract

Nanohybrids were fabricated from a poly(L-lactic acid) solution loaded with various concentrations of organically modified montmorillonite. Investigation of the produced composites' morphology by X-ray diffraction analysis, transmission electron microscopy and atomic force microscopy revealed a coexistence of intercalated and exfoliated clay particles, with the latter ones being predominant for low filler loadings. Porous scaffolds of pure and nanocomposite poly(L-lactic acid) were prepared using supercritical CO_2 as antisolvent and the influence of montmorillonite content was examined. It was observed that the final cellular structure was strongly related to the filler content.

Keywords: Nanocomposites; Scaffolds; Supercritical CO_2

1. Introduction

Biodegradable and biocompatible polymers, which can be used in various biomedical applications, are of great scientific interest today. Poly(L-lactic acid) (PLLA) is a biodegradable aliphatic polyester derived from renewable resources and is considered to be one of the most promising such polymers. It is extensively used in tissue engineering for treating patients suffering from damaged or lost organ or tissue [1].

Tissue engineering is aiming, primarily, at the regeneration of damaged tissue. This task demands a combination of molecular biology and materials engineering, since in many applications a scaffold is needed to provide a temporary artificial matrix for cell seeding. In general, scaffolds must meet certain specifications such as high porosity, proper pore size, biocompatibility, biodegradability and proper degradation rate [2]. Furthermore, the scaffold must provide sufficient mechanical support to maintain stresses and loadings generated during in vitro or in vivo regeneration [1,2]. Due to the broad potential uses of tissue-engineered systems, there is a continuous search for scaffold materials that exhibit suitable properties that can be tailored to several tissue systems.

In this direction, nanostructured hybrid organic/inorganic composites have attracted considerable attention in many areas of polymer applications. Introduction of small quantities of high aspect ratio nano-sized silicate particles can significantly improve mechanical and physical properties of the polymer matrix [3]. Recently Lee et al. prepared nanocomposite PLLA using a solution casting technique [4]. Using this material, they prepared scaffolds by a salt leaching method. They concluded that the incorporation of the clay mineral dramatically enhances the tensile modulus of the scaffolds up to 40%.

However, many agents like the pore structure, the porosity, the crystallinity and the degradation rate may alter the mechanical properties and, thus, the efficiency of a scaffold. As a consequence, the scaffold fabrication method should allow for the control of its pore size and shape and should enhance the maintenance of its mechanical properties and materials' biocompatibility [1,2].

* Corresponding author. Tel.: +30 2310 996223; fax: +30 2310 996232.
E-mail address: cpanayio@auth.gr (C. Panayiotou).

0032-3861/$ - see front matter © 2007 Elsevier Ltd. All rights reserved.
doi:10.1016/j.polymer.2007.08.021

During the past years many techniques have been applied for making porous PLLA scaffolds. Among the most popular are porogen leaching [5], temperature induced phase separation [6], and phase inversion in the presence of a liquid non-solvent [7]. On the other hand, foaming of polymers using supercritical fluids is a versatile method in obtaining porous structures [2,8]. Nevertheless, this technique is applied more in amorphous polymers. In semicrystalline polymers such as PLLA, it is rather difficult to obtain uniform porous structures with the gas foaming technique at temperatures much lower than the melting point [2,9,10].

Supercritical CO_2, as an antisolvent, has been extensively used for the production of microparticles and the encapsulation of drugs into biodegradable polymer matrices [11]. In contrast, rather few experiments have been made for the production of porous structures. Among them is the production of porous polystyrene, polycarbonate, nylon 6, and cellulose acetate membranes [12–15].

Phase inversion using supercritical antisolvent is analogous to traditional phase inversion with immersion precipitation. This technique consists of immersing a thin film of the polymer solution in a bath containing a non-solvent (with respect to the polymer). The addition of the non-solvent causes thermodynamic instability resulting in phase separation. The properties of the final structure are mainly controlled by the precipitation temperature, the strength of the non-solvent bath and the composition of the casting solution. The use of a supercritical fluid as an antisolvent allows for the tuning of the antisolvent strength simply by regulating the pressure.

In our previous work, the role of nanostructure on the thermo-mechanical properties of PLLA was investigated [16]. Furthermore, we explored the use of supercritical CO_2 as antisolvent for the production of porous PLLA matrices. The effect of temperature, pressure and initial solution concentration on the final porous structure was investigated [10]. In this study, porous structures of pure and nanocomposite PLLA were prepared by the same technique and the effect of clay content was investigated.

2. Experimental section

2.1. Materials

PLLA ($M_n = 81\,000$, $M_w/M_n = 1.9$, and 0% content in D-lactide stereoisomer) was obtained from Galactic S.A., chloroform and dichloromethane (>99.9% purity) from Fluka Chemie and CO_2 from Air Liquide Mediterranée (>99.98% purity). All materials were used without any further purification. Organically modified montmorillonite (C_{16}MMT) was prepared with an ion-exchange reaction between sodium montmorillonite (NaMMT) (CEC = 92.6 meq/100 g clay) and excess of hexadecylammonium salt [16]. The organophilic clay was then dried under vacuum at 75 °C for 24 h and was ground in order to obtain a powder form (the average size of the clay particles was less than 15 μm).

2.2. Preparation of nanocomposites and porous structures

Nanocomposites were prepared by the solvent casting technique. The organomodified mineral was initially dispersed in chloroform. The clay suspension was sonicated for 1 h with a Heat Systems – Ultrasonics, Inc. W-375 sonicator. Then, the polymer was dissolved and the mixture was further sonicated for 1 h. The mixture was then cast onto Petri dishes and kept in a chloroform atmosphere achieving a slow solvent evaporation. The received films were further dried in vacuum at 50 °C for 24 h. Chloroform was selected as the PLLA solvent for the hybrids' preparation, due to its low vapor pressure compared to dichloromethane. Slow solvent evaporation leads to a more homogeneous film formation [17].

The experimental apparatus was described in a previous work, where the effect of experimental conditions such as temperature and pressure on the final porous structure of neat PLLA was investigated [10]. Solutions of pure PLLA and C_{16}MMT-reinforced PLLA in dichloromethane (15% w/v) were prepared and a small quantity (approx. 1.5 mL) was placed in a vessel (stainless steel cap with 1.7 cm diameter) inside the high-pressure cell (internal volume 40 mL). The cell was immediately filled with supercritical CO_2. It remained at 165 bar and 45 °C for 2.5 h. In this pressure and temperature supercritical CO_2 is fully miscible with dichloromethane [18], while in the same conditions porous structures of neat PLLA were successfully produced in a previous work [10]. Then, the cell was flushed by adding fresh CO_2 at the same conditions of pressure and temperature, in order to extract the residual organic solvent. In this step, CO_2 was added at a constant flow rate (approx. 0.4 g/min) for 2.5 h. Then, the system was depressurized very slowly and with a constant rate of 1 bar/min. That way, porous structures with clay loadings of 0 wt%, 1 wt%, 3 wt%, 5 wt%, and 9 wt% were formed.

The effect of the mineral clay content on the final porous structure was investigated through a series of experiments where all the parameters, but the clay content, were kept constant. Thus, the pressure was kept at 165 bar, the temperature at 45 °C and the initial solution concentration was 15% w/v.

Furthermore, the ability of CO_2 to foam pure or nanocomposite PLLA at temperatures far below the melting point was investigated in order to eliminate the contingency that another process (different than the phase inversion due to the addition of the supercritical non-solvent) might alter the porous structure after initial pore formation. Dense films of pure and nanocomposite PLLA were exposed to CO_2 at 230 bar and 45 °C for 10 h. Then, the system was rapidly depressurized over 2 min. None of the samples exhibited any evidence of foaming.

2.3. Characterization

The structure of the nanohybrids produced was investigated by X-ray diffraction (XRD) analysis using a Siemens D-500 diffractometer and Ni-filtered Cu Kα radiation

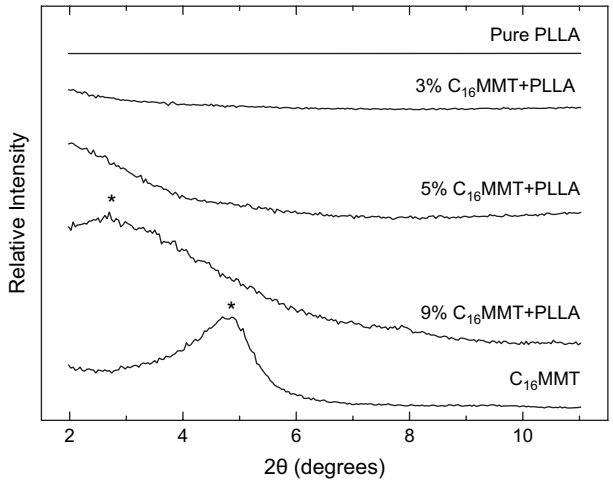

Fig. 1. X-ray diffraction patterns of PLLA nanocomposites with various loadings of the organophilic clay.

($\lambda = 0.154$ nm). The scanning range was varied from $2\theta = 2°$ to 11°.

Transmission electron microscopy (TEM) bright field imaging was performed using a Jeol 120CX microscope operating at 120 kV. The samples were initially mechanically thinned down to 10 μm. Further thinning to electron transparency was achieved by Ar^+ ion beam milling at a low incident angle of 5°.

The dispersion of the silicate layers into the matrix was also evaluated by atomic force microscopy (AFM) using a Veeco, CP-II microscope. A commercial silicon tip-cantilever was used with a spring constant of 20–80 N/m, a resonance frequency in the 200–400 kHz range and a tip radius of curvature of less than 10 nm. Topography and phase images were recorded in tapping mode at room temperature and ambient atmosphere. The samples were microtomed before use in order to obtain smooth cross-sections, which are necessary for detailed observations. The recorded images were analyzed using SPM Lab software provided by the manufacturer.

The porous samples were fractured in liquid nitrogen and their cross-sections were examined by scanning electron microscopy (SEM, mod. JEOL, JSM-840A). All surfaces were coated with graphite to avoid charging under the electron beam. The pore size distributions were obtained using appropriate image analysis software.

The densities of the foamed samples were measured by the buoyancy method (ASTM D-792) with triethylene glycol as the liquid with the known density. There was no obvious liquid uptake by the foamed samples, which if happened, would bias the measurements.

Crystallinity and melting point of the unfoamed compression-molded discs were determined with differential scanning calorimetry (Shimadzu DSC-50). The polymer exhibited glass to rubber transition around 55.4 °C, recrystallization point at 107 °C, melting point at 176.2 °C and 34% crystallinity [16]. Crystallinity was calculated assuming that the heat of fusion of the 100% crystalline material is equal to 93 J/g [19].

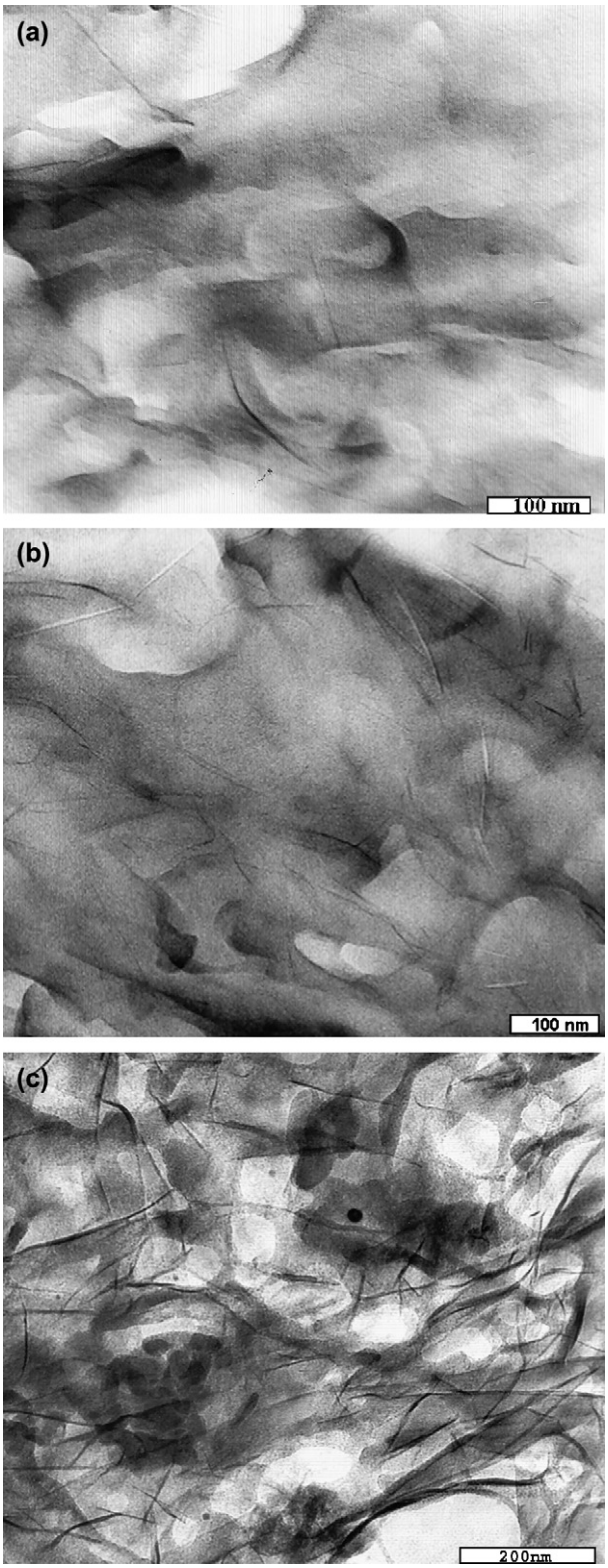

Fig. 2. TEM micrograph depicting the structure of PLLA with 3 wt% (a), 5 wt% (b), and 9 wt% (c) of organomodified montmorillonite.

3. Results and discussion

Fig. 1 presents the XRD patterns of pure and nanocomposite PLLA. The initial peak at 4.85° (corresponding to

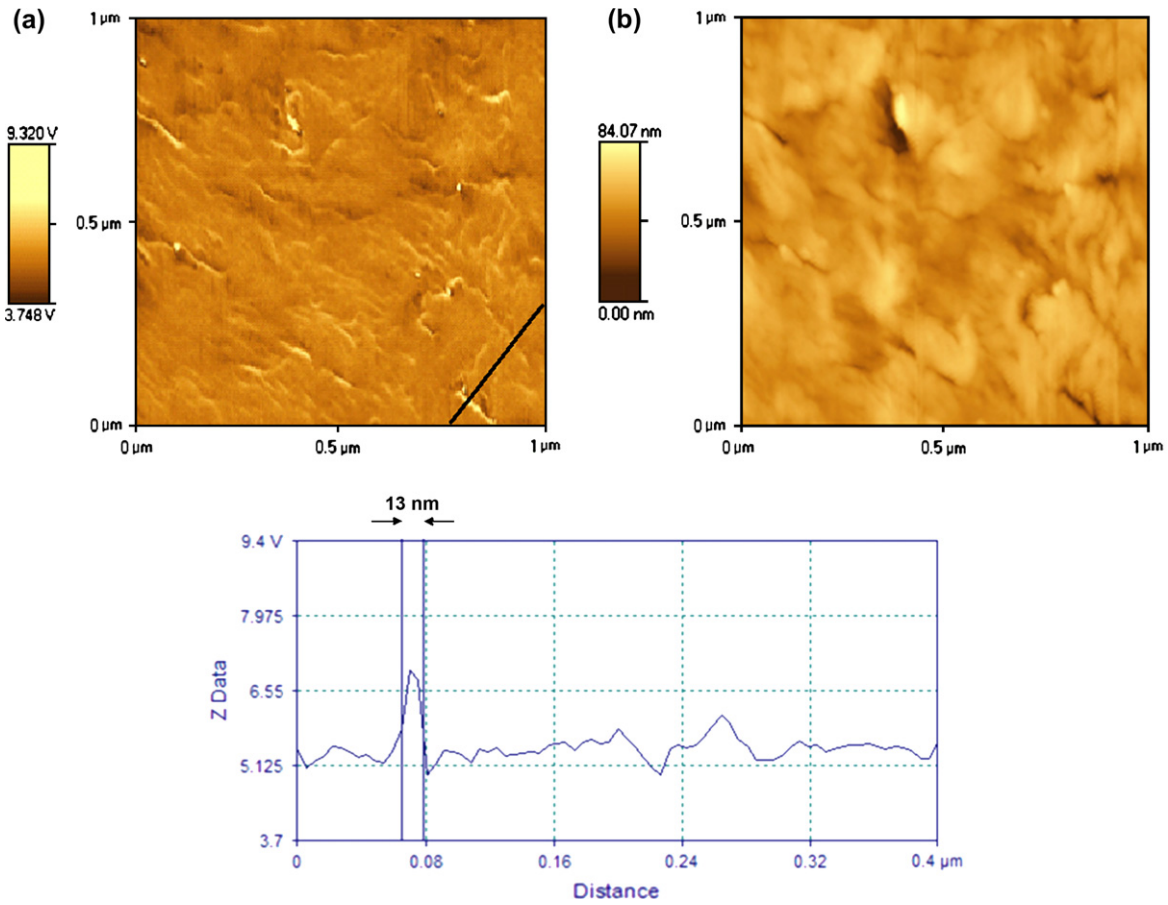

Fig. 3. Top: AFM phase (a) and topography (b) images of an exfoliated PLLA nanocomposite (containing 3 wt% C_{16}MMT). Bottom: profile across the black line in image (a); assuming that the tip radius of curvature is around 6 nm, the real particle thickness approaches 1 nm.

$d_{(001)} = 1.82$ nm) of the organomodified montmorillonite was replaced by a broader peak at 2.7° ($d_{(001)} = 3.27$ nm) in the case of the 9 wt% nanocomposite indicating that the polymer chains diffused into the silicate galleries expanding the clay structure. The broadening of the peak, which may be the result of superposition of reflections that correspond to various interlayer distances, implies a partial disorder in the parallel stacking of the clay and a possible existence of some exfoliated clay layers. There was no peak being detected for clay loadings less than 5 wt% suggesting that exfoliation of the clay platelets took place.

The structure of PLLA nanocomposites was observed by TEM. Fig. 2 illustrates the morphology of nanocomposites prepared with the addition of 3 wt% (a), 5 wt% (b), and 9 wt% (c) of organomodified clay. Dark lines represent the cross-sections of the clay layers and the gray area corresponds to the matrix. In all the cases, nano-sized clay particles are randomly dispersed in the polymer matrix. However, as the clay loading decreases the exfoliated silicate sheets' percent increases.

AFM observations were also performed in order to investigate the dispersion of the organoclay in PLLA. Fig. 3 describes the morphology of a hybrid prepared by the addition of 3 wt% organoclay. A profile line analysis was used to determine the size of the particles presented in image 3(a) as lighter areas. The raw data show that the thickness of the marked thin light region is around 13 nm. Considering that the tip used for taking the AFM images was certified by its manufacturer to have a radius of curvature (roc) < 10 nm, it appears that the real thickness of the specific filler particle is of the order of 1 nm. This indicates that the light phase variations of 3(a) phase image are exfoliated clay platelets dispersed into the polymer matrix. On the contrary, phase and height shift image analysis of PLLA with 9 wt% C_{16}MMT revealed the existence of intercalated clay tactoids (Fig. 4).

Both the AFM and the TEM data show that at low clay content exfoliation predominates. Increase of the filler loading results in relatively more delaminated individual particles. However, when the clay content exceeds 5 wt%, complete exfoliation of such high aspect ratio silicate particles is obstructed due to the limited area remaining available in the polymer matrix and thus, the degree of intercalation increases [20].

The morphology of the porous structures formed by phase inversion depends on various thermodynamic and kinetic factors, as well. Consequently, the qualitative analysis of the results becomes rather involved. As it has been reported [7,10,14], in semicrystalline polymers the phase inversion proceeds along with two competitive phenomena: Liquid–Liquid (L–L) and Solid–Liquid (S–L) demixing. The former leads

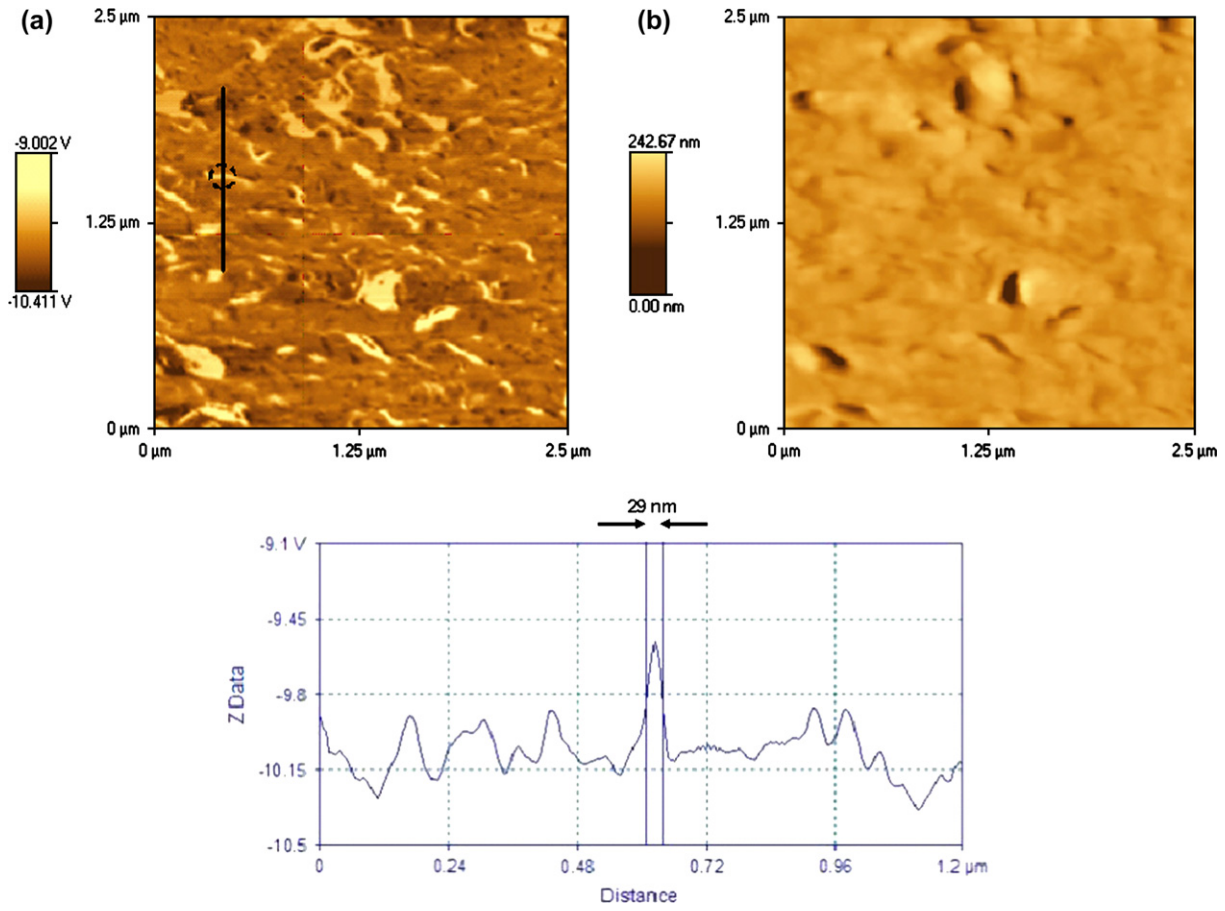

Fig. 4. Top: AFM phase (a) and topography (b) images of a PLLA nanocomposite (containing 9 wt% C_{16}MMT). Bottom: profile across the black line in image (a). The light areas in the phase image represent intercalated clay tactoids.

to uniform cellular structures, while the latter results in spiny or jagged structures that are more interconnected. Usually the final result is the product of simultaneous L–L and S–L demixing and the dominant mechanism is not always the thermodynamically favored one [14]. In general, the L–L demixing proceeds rapidly and can precede the S–L demixing even when the latter is thermodynamically favored [21].

In all cases presented in Figs. 5 and 6c, structures with uniform cross-sections and cellular pores were obtained. This indicates L–L demixing as the dominant mechanism. The pores are formed due to the initial nucleation and growth of the polymer-lean phase that occurs inside the polymer-rich phase. The diffusion of the solvent to the polymer-lean phase causes the crystallization of the polymer-rich phase and subsequently the ''locking'' of the cellular structure.

Comparison of Fig. 5a with Fig. 5b–e shows a great difference between the neat PLLA and nanocomposite porous materials. The pure polymer (Fig. 5a) exhibits a more jagged structure with pores that are more interconnected. On the contrary, the addition of clay (Fig. 5b–e) results in more uniform cellular structures with larger pores, which have a more pronounced spherical size. The latter observation indicates that the L–L demixing is more dominant in the case of nanocomposite materials.

In all cases, on the top surface of the porous samples large spherical structures were formed. Fig. 6a and b present such formations for neat PLLA and the 3 wt% nanocomposite, respectively. Similar structures have also been observed in porous PLLA membranes prepared by immersion precipitation and were recognized as spherulites [7]. Their presence is attributed to the rapid exchange of solvent with non-solvent immediately after immersion. This exchange causes a rapid increase in the polymer concentration at the top surface facilitating the crystallization. In all cases, the size of these structures was greater in nanocomposite materials than in the neat polymer.

The effect of the clay content on the pore size distribution and on the bulk foam density is shown in Figs. 7 and 8, respectively. As shown in Fig. 7, the addition of a small amount of clay (1 wt%) resulted in a great increase of the pore size. The average diameter increased from 49.5 μm (neat polymer) to 201.7 μm. Further increase of the clay content from 1 wt% to 5 wt% decreased the size of pores, while addition of clay for a total 9 wt% did not influence the cell size. In contrast, the bulk foam density was not influenced by the increase of the clay content from 1 wt% to 9 wt% (Fig. 8).

In such a complex process, the final pore size reflects the net effect of several factors and a number of hypotheses could

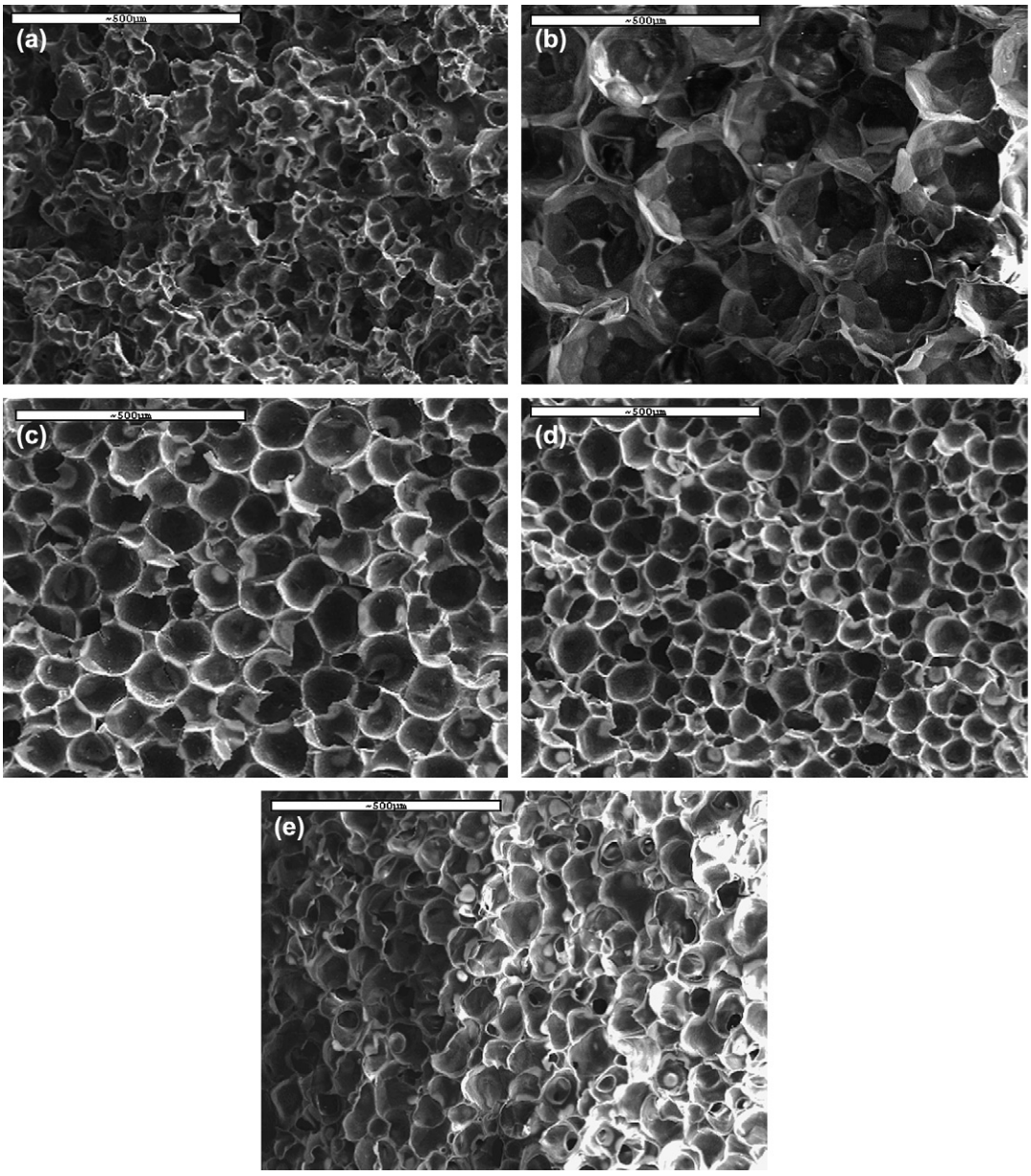

Fig. 5. Cross-sections of the porous samples, clay content: (a) 0 wt%, (b) 1 wt%, (c) 3 wt%, (d) 5 wt%, and (e) 9 wt%.

be explored as potential explanations. Firstly, the addition of clay platelets could enhance the heterogeneous nucleation of the polymer-lean phase droplets. This favors the formation of more pores with smaller size. Secondly, the addition of the inorganic filler could enhance the overall crystallization rate via heterogeneous nucleation, if the crystallites' nucleation rate is the step that controls this process. On the contrary, if the crystal growth rate controls the overall crystallization rate, the addition of the clay could decelerate crystallization due to the viscosity increase. As the crystallization rate decreases, the solidification and subsequently the ''locking'' of the porous structure is delayed. As a consequence, the L–L demixing occurs for a longer time period and the polymer-lean phase has more time to grow.

To the best of authors' knowledge, the crystallization kinetics of polymer nanocomposites from solution under supercritical CO_2 atmosphere has not been studied. Recently, Lee et al. [4] studied the thermal properties of PLLA nanocomposites. They indicated that the addition of small amount of inorganic filler reduced the crystallization and the melting temperature as well as the overall crystallinity. The authors explained their observations by suggesting that the clay platelets act as nucleation sites favoring heterogeneous crystallization (thus, decreased crystallization temperature) and facilitating the production of more and thinner crystallites (thus, decreased melting temperature).

Krikorian and Pochan have studied the kinetics of isothermal crystallization in PLLA nanocomposite melts [22,23]. They claimed that when the clay organic modifier is highly miscible with PLLA, the dominating exfoliation results in slower bulk crystallization rate compared to that of the neat polymer. This is happening because high miscible clay

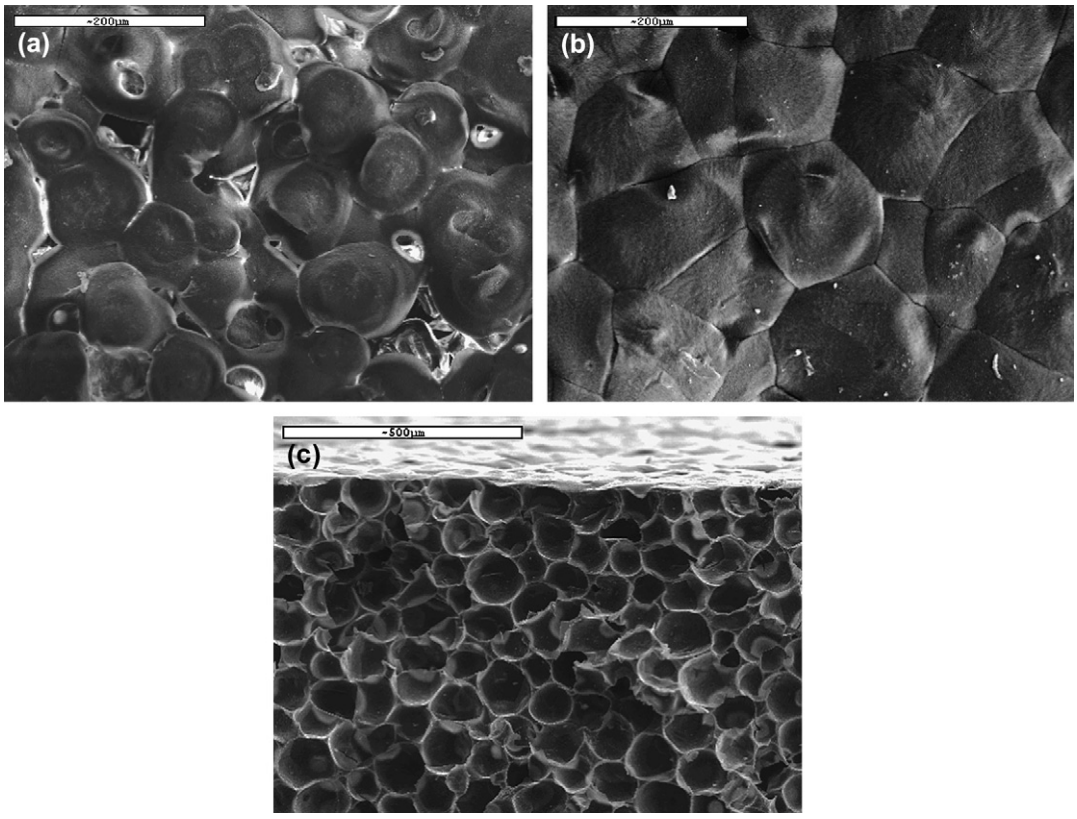

Fig. 6. Top surface (skin) of (a) pure polymer, (b) nanocomposite (3 wt% clay content), and (c) upper side of the cross-section (3 wt% clay content).

platelets hinder the interchain interactions, which are vital for crystal nuclei formation. In addition, the spherulitic nucleation rate is lower but the spherulite radial growth rate is higher. Low spherulitic nucleation coupled with higher radial growth rate results in spherulites with larger size. In contrast, when the miscibility between the polymer and the organic clay modifier is lower, an intercalated structure is more possible. In that case, the clay acts as an effective nucleation agent leading to increased bulk crystallization rates and to the formation of more spherulites with much smaller size. In both cases, the degree of crystallinity is lower than that of the pure polymer.

In our case, we have exfoliated clay particles for clay loadings less than 5 wt%. It is possible that these exfoliated structures decrease the overall crystallization rate in the nanocomposite materials compared with that of the neat polymer. As a consequence, the polymer-lean phase has more time to grow before the polymer-rich phase solidifies and thus, the formation of larger pores with more pronounced cellular shape is favored.

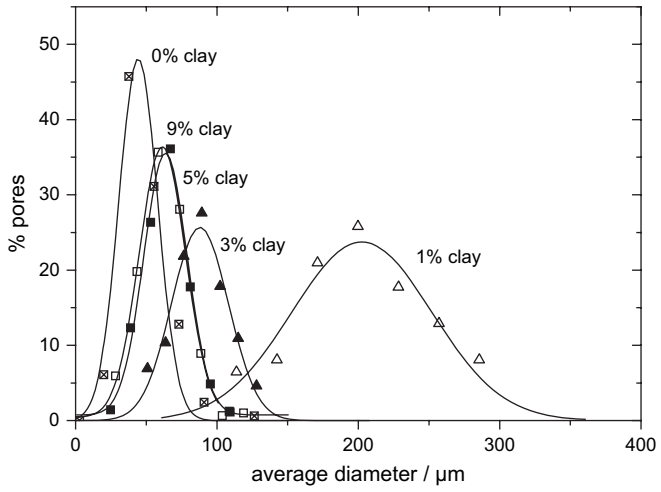

Fig. 7. Effect of the clay content on the average pore size.

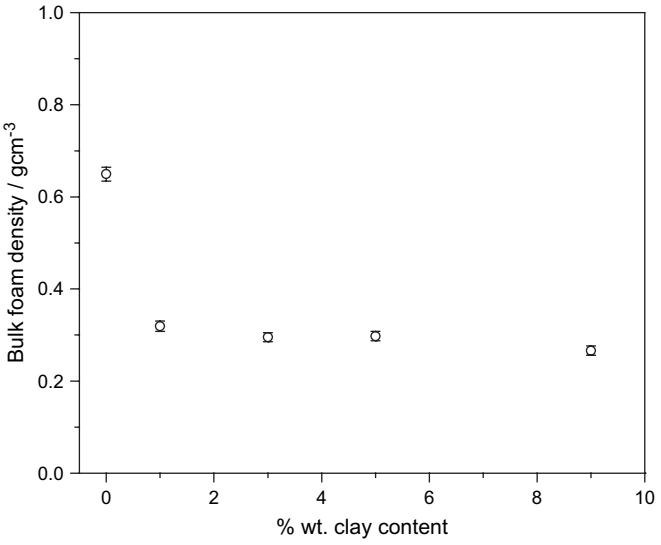

Fig. 8. Effect of the clay content on the bulk foam density.

Finally, the decrease of pore size that was observed as the clay content increased from 1 wt% to 5 wt% could be attributed to the heterogeneous nucleation of polymer-lean phase droplets that led to the formation of more pores and thus, with smaller size.

4. Conclusions

In this work, the potential of fabricating porous nanohybrid PLLA structures was explored. Initially, nanocomposites were prepared from a poly(L-lactic acid) solution loaded with various concentrations of organically modified montmorillonite. Investigation of their morphology by X-ray diffraction, transmission electron microscopy, and atomic force microscopy revealed the coexistence of intercalated and exfoliated clay particles, with the latter ones being the predominant for low loadings (typically less than 5 wt%).

Subsequently, cellular structures were prepared using supercritical CO_2 as antisolvent and the influence of the clay content was investigated. The analysis of the results showed that the introduction of a small amount of the organically modified mineral clay has a major effect on the final porous structure. Contrary to the pure polymer, all the nanocomposite materials exhibited more uniform cellular structures with large pores. This was probably due to the influence of the clay in the crystallization behavior of the nanocomposite material.

Fabrication of porous structures that could be used as scaffolds in tissue engineering includes (a) the reinforcement of the polymer matrix and control of the mechanical properties, (b) the preparation of structures with fine cellular, interconnected pores with narrow size distribution, (c) the ability of tailoring the pore size for different applications, and (d) the ability of encapsulating pharmaceutical substances inside the matrix. This work along with our previous one, where the ability of tailoring the pore size simply by changing the experimental conditions was studied [10], covers many of the previous tasks. Topics that need further investigation are the potential of using phase inversion with supercritical CO_2 for the encapsulation of pharmaceutical substances inside the scaffolds and the modification of the method for the enhancement of the interconnection of the pores.

Acknowledgment

The partial financial support of the Greek State (Ministry of Education) and the European Union through the research grant Archimedes (MIS 86383) is gratefully acknowledged.

References

[1] Ma PX. Mater Today 2004;7(5):30–40.
[2] Quirk RA, France RM, Shakesheff KM, Howdle SM. Curr Opin Solid State Mater Sci 2004;8(3–4):313–21.
[3] Ray SS, Okamoto M. Prog Polym Sci 2003;28(11):1539–641.
[4] Lee JH, Park TG, Park HS, Lee DS, Lee YK, Yoon SC, et al. Biomaterials 2003;24(16):2773–8.
[5] Chen GP, Ushida T, Tateishi T. Mater Sci Eng C 2001;17(1–2):63–9.
[6] Nam YS, Park TG. Biomaterials 1999;20(19):1783–90.
[7] Van de Witte P, Esselbrugge H, Dijkstra PJ, Van den Berg JWA, Feijen J. J Membr Sci 1996;113(2):223–36.
[8] Goel SK, Beckman EJ. Polym Eng Sci 1994;34(14):1137–47.
[9] Doroudiani S, Park CB, Kortschot MT. Polym Eng Sci 1996;36(21):2645–62.
[10] Tsivintzelis I, Pavlidou E, Panayiotou C. J Supercrit Fluids 2007;40(2):317–22.
[11] Tomasko DL, Li H, Liu D, Han X, Wingert MJ, Lee LJ, et al. Ind Eng Chem Res 2003;42(25):6431–56.
[12] Matsuyama H, Yano H, Maki T, Teramoto M, Mishima K, Matsuyama K. J Membr Sci 2001;194(2):157–63.
[13] Kim MS, Lee SJ. J Supercrit Fluids 2004;31(2):217–25.
[14] Kho YW, Kalika DS, Knutson BL. Polymer 2001;42(14):6119–27.
[15] Reverchon E, Cardea S. J Membr Sci 2004;240(1–2):187–95.
[16] Marras SI, Zuburtikudis I, Panayiotou C. Eur Polym J 2007;43(6):2191–206.
[17] Strawhecker KE, Kumar SK, Douglas JF, Karim A. Macromolecules 2001;34(14):4669–72.
[18] Tsivintzelis I, Missopolinou D, Kalogiannis K, Panayiotou C. Fluid Phase Equilib 2004;224(1):89–96.
[19] Rusa CC, Tonelli AE. Macromolecules 2000;33(15):5321–4.
[20] Paul MA, Alexandre M, Degee P, Calberg C, Jerome R, Dubois P. Macromol Rapid Commun 2003;24(9):561–6.
[21] Van de Witte P, Dijkstra PJ, Van den Berg JWA, Feijen J. J Membr Sci 1996;117(1–2):1–31.
[22] Krikorian V, Pochan DJ. Macromolecules 2004;37(17):6480–91.
[23] Krikorian V, Pochan DJ. Macromolecules 2005;38(15):6520–7.